

Glueballs, a fulfilled promise of QCD?

Eberhard Klempt

Helmholtz-Institut für Strahlen- und Kernphysik, Universität Bonn, Germany

Received: December 29, 2022/ Revised version:

Abstract. This is a contribution to the review “50 Years of Quantum Chromodynamics” edited by F. Gross and E. Klempt, to be published in EPJC. The contribution remembers the early searches and explains how to find a glueball, based on its properties. The results of a coupled-channel analysis are presented that provides evidence for the scalar glueball and first hints for the tensor glueball. Data on radiative decays of $\psi(2S)$ and $\Upsilon(1S)$ show scalar intensity that is likely due to glueball production.

1 Introduction

At the *Workshop on QCD: 20 Years Later* held 1992 in Aachen, Heusch [1] reported on searches for glueballs, gluonium, or glue states as Fritzsche and Gell-Mann [2,3] had called this new form of matter. Glueballs are colorless bound states of gluons and should exist when their newly proposed quark-gluon field theory yields a correct description of the strong interaction. The title of Heusch’s talk *Gluonium: An unfulfilled promise of QCD?* expressed the disappointment of a glueball hunter: At that time there was some - rather weak - evidence for glueball candidates but there was no convincing case. In 1973, the e^+e^- storage ring SPEAR at the Stanford Linear Accelerator Center had come into operation and one year later, the J/ψ resonance was discovered [4] - this was the very first SPEAR publication on physics. The J/ψ resonance and its radiative decay became and still is the prime reaction for glueball searches.

One of the first glueball candidates was the $\iota(1440)$ [5,6]. The name ι stood for the “number one” of all glueballs to be discovered. It was observed as very strong signal with pseudoscalar quantum numbers in the reaction $J/\psi \rightarrow \gamma K \bar{K} \pi$. Its mass was not too far from the bag-model prediction (1290 MeV) [7]. Now the $\iota(1440)$ is supposed to be split into two states, $\eta(1405)$ and $\eta(1475)$, where the lower-mass meson is still discussed as glueball candidate even though its mass is incompatible with lattice gauge calculations. They find the mass of the pseudoscalar glueball above 2 GeV.

A second candidate was a resonance called $\Theta(1640)$ [8,9]. It was seen in the reaction $J/\psi \rightarrow \gamma \eta \eta$ and confirmed - as $G(1590)$ - by the GAMS collaboration in $\pi^- p \rightarrow \eta \eta n$ [10]. Its quantum numbers shifted from $J^{PC} = 2^{++}$ to 0^{++} , and its mass changed to 1710 MeV. This resonance still plays an important role in the glueball discussion.

A third candidate, or better three candidates, were observed in the OZI rule violating process $\pi^- p \rightarrow \phi \phi n$

[11,12]. Three $\phi\phi$ resonances at 2050, 2300 and 2350 MeV were reported. I remember Armenteros saying: *When you have found one glueball, you have made a discovery. When you find three, you have a problem.* Now I believe that this was a very early manifestation of the tensor glueball.

The situation was not that easy at that time as described here. Nearly for each observation, there were contradicting facts, and Heusch concluded his talk at the QCD workshop with the statement: *there is no smoking-gun candidate for gluonium* At this workshop, I had the honor to present the results of the Crystal Barrel experiment at LEAR and to report the discovery of two new scalar mesons, $f_0(1370)$ and $f_0(1500)$, and I was convinced, Heusch was wrong: $f_0(1500)$ was the glueball! And I turned down my internal critical voice which told me that in my understanding of $\bar{p}N$ annihilation, this process is not particularly suited to produce glueballs [13,14]. Our glueball $f_0(1500)$ was not seen in radiative J/ψ decays where a glueball should stick out like a tower in the landscape. The $f_0(1500)$ as scalar glueball? That could not be the full truth!

2 QCD predictions

2.1 Glueball masses

First estimates of the masses of glueballs were based on bag models. The color-carrying gluon fields were required to vanish on the surface of the bag. Transverse electric and transverse magnetic gluons were introduced populating the bag. The lowest excitation modes were predicted to have quantum numbers $J^{PC} = 0^{++}$ and 2^{++} and to be degenerate in mass with $M = 960$ MeV [7,15]. A very early review can be found in Ref. [16].

The bag model is obsolete nowadays. Most reliable are presumably simulation of QCD on a lattice (see Ref. [25] for an introduction). In lattice gauge theory, the spacetime is rotated into an Euclidean space by the transformation

Table 1. Masses of low-mass glueballs, in units of MeV. Lattice QCD results are taken from Refs. [17, 18] (quenched) and Ref. [19] (unquenched). Szczepaniak and Swanson [20] construct of a quasiparticle gluon basis for a QCD Hamiltonian. Results from QCD sum rule results are given in Ref. [21], from using Dyson-Schwinger equations in [22, 23], and from a graviton-soft-wall model in Ref. [24].

Glueball	Ref. [17]	Ref. [18]	Ref. [19]	Ref. [20]	Ref. [21]	Ref. [22]	Ref. [24]
$ 0^{++}\rangle$	$1710 \pm 50 \pm 80$	1653 ± 26	1795 ± 60	1980	1780^{+140}_{-170}	1850 ± 130	1920
$ 2^{++}\rangle$	$2390 \pm 30 \pm 120$	2376 ± 32	2620 ± 50	2420	1860^{+140}_{-170}	2610 ± 180	2371
$ 0^{-+}\rangle$	$2560 \pm 40 \pm 120$	2561 ± 40	–	2220	2170 ± 110	2580 ± 180	

$t \rightarrow it$ and then discretized into a lattice with sites separated by a distance in space and time. The gauge fields are defined as links between neighboring lattice points, closed loops of the link variables (Wilson loops) allow for the calculation of the action density. Technically, gluons on a space-time lattice struggle against large vacuum fluctuations of the correlation functions of their operators, the signal-to-noise ratio falls extremely rapidly as the separation between the source and sink is increased. These difficulties can be overcome by anisotropic spacetimes with coarser space and narrow time intervals [17, 26]. Fermion fields are defined at lattice sites. Different techniques have been developed to include fermions in lattice calculations [18]. The effect of sea quarks on glueball masses seems to be small [19].

Recently, a number of different approaches were chosen to approximate QCD by a model that is solvable analytically. Szczepaniak and Swanson [20] constructed a quasiparticle gluon basis for a QCD Hamiltonian in Coulomb gauge that was solved analytically. A full glueball spectrum was calculated with no free parameter. The authors of Ref. [21] constructed relativistic two- and three-gluon glueball currents and applied them to perform QCD sum rule analyses of the glueball spectrum. The Gießen group calculated masses of ground and excited glueball states using a Yang-Mills theory and a functional approach based on a truncation of Dyson-Schwinger equations and a set of Bethe-Salpeter equations derived from a three-particle-irreducible effective action [22, 23].

AdS/QCD relies on a correspondence between a five dimensional classical theory with an AdS metric and a supersymmetric conformal quantum field theory in four dimensions. In the bottom-up approach, models with appropriate operators are constructed in the classical AdS theory with the aim of resembling QCD as much as possible. Confinement is generated by a hard wall cutting off AdS space in the infrared region, or spacetime is capped off smoothly by a soft wall to break the conformal invariance. Rinaldi and Vento [24] calculated the glueball mass spectrum within AdS/QCD. The results on glueball masses are summarized in Table 1.

2.2 The width of glueballs

Glueballs are often assumed to be narrow. ϕ decays into $\rho\pi$ are suppressed since the primary $s\bar{s}$ pair needs to annihilate and a new $q\bar{q}$ pair needs to be created. In glueball

decays, there is no pair to be annihilated but a $q\bar{q}$ pair needs to be created. If the OZI rule suppresses the decay by a factor 10 to 100, we might expect the width of glueballs to be suppressed by a factor 3 to 10. Assuming a “normal” width of 150 MeV, a glueball at 1600 MeV could have a width of 15 to 50 MeV. This argument is supported by arguments based on the $1/N_c$ expansion (see, e.g., Ref. [27]).

Narison applied QCD sum rules [28]. Assuming a mass of 1600 MeV, he calculated the 4π width of the scalar glueball to 60 to 138 MeV while the partial decay width of the tensor glueball at 2 GeV to pseudoscalar mesons should be less than 155 MeV. Calculations on the lattice gave a partial decay width for decays into pseudoscalar mesons of 108 ± 29 MeV for a scalar glueball mass of 1700 MeV [29]. In a semi-phenomenological model, Burakovsky and Page find that the width of the scalar glueball (at 1700 MeV) should exceed 250 to 390 MeV. A flux tube model predicted the mass of the glueball of lowest mass to 1680 MeV and its width to 300 MeV [30]. In a field theoretical approach with an effective Coulomb gauge the glueball width was estimated to 100 MeV [31].

2.3 Radiative yields

The study of radiative decays of the J/ψ meson is the prime path to search for glueballs with masses of less than ~ 2500 MeV.

Gui *et al.* [32] calculated the yield of a scalar glueball having a mass of 1710 MeV on lattice and found

$$BR_{J/\psi \rightarrow \gamma G_{0^{++}}}(TH) = (3.8 \pm 0.9) \cdot 10^{-3}. \quad (1)$$

For higher glueball masses the yield increases.

Narison gave a mass dependent formula derived from sum rules. For a mass of 1865 MeV, a yield of about 10^{-3} is predicted [28].

The tensor glueball is expected [33] to be observed with a branching ratio

$$BR_{J/\psi \rightarrow \gamma G_{2^{++}}}(TH) = (11 \pm 2) \cdot 10^{-3}. \quad (2)$$

Production of the pseudoscalar glueball seems to be considerably smaller. For a mass of 2395 (or 2560) MeV, the authors of Ref. [34] find

$$BR_{J/\psi \rightarrow \gamma G_{0^{-+}}}(TH) = (0.231 \pm 0.080) \cdot 10^{-3} \\ \text{or} = (0.107 \pm 0.037) \cdot 10^{-3}. \quad (3)$$

These are very significant yields, and the glueballs must be found provided they can be identified convincingly as glueballs amidst their $q\bar{q}$ companions.

3 How to identify a glueball

Figure 1 shows the prime reactions in which glueballs have been searched for.

3.1 $N\bar{N}$ annihilation

A decisive step forward in the search for glueballs was the discovery of two scalar isoscalar states in $\bar{p}p$ annihilation at rest. With the large statistics available at the Low Energy Antiproton Ring (LEAR) at CERN, $f_0(1370)$ and $f_0(1500)$ were identified in several final states. A large fraction of the data taken at LEAR is still used jointly with data on radiative J/ψ decays in a coupled-channel analysis. Glueballs decay via $q\bar{q}$ pair creation. Hence they can be produced via $q\bar{q}$ annihilation. Meson production in $\bar{p}p$ annihilation was studied by the ASTERIX, OBELIX and Crystal Barrel experiments at LEAR and is a major objective of the PANDA collaboration at the GSI.

3.2 Central production

In central production, two hadrons (e.g. two protons) scatter in forward direction via the exchange of Pomerons. Pomerons are supposed to be glue-rich, hence glueballs can be formed in Pomeron-Pomeron fusion. This process was studied extensively at CERN by the WA76 and WA102 collaborations and is now investigated with the STAR detector at BNL. In the WA102 experiment, $f_0(1370)$ and $f_0(1500)$ were confirmed and $f_0(1710)$ was added to the number of scalar resonances.

3.3 radiative J/ψ decays

In radiative J/ψ decays, the primary $c\bar{c}$ pair converts into two gluons and a photon. The two gluons are mainly produced in S -wave, the two gluons can form scalar and tensor glueballs which should be produced abundantly. The large statistics available from BESIII at Beijing makes this reaction the most favorable one for glueball searches. Radiative decays of heavy mesons is the only process for which glueball yields have been calculated. The data will be discussed below in more detail.

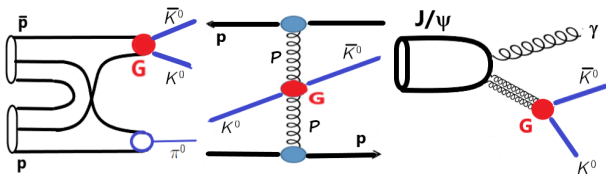


Fig. 1. Reactions most relevant for glueball searches. Left: $\bar{p}p$ annihilation; middle: Pomeron-Pomeron fusion; right: radiative J/ψ decays. The glueball is supposed to decay into $K^0 \bar{K}^0$.

3.4 Decay analysis

The decay of mesons into two pseudoscalar mesons is governed by $SU(3)_F$. In a meson nonet, there are two isoscalar mesons, one lower in mass the other one higher, which both contain a $n\bar{n} = (u\bar{u} + d\bar{d})/\sqrt{2}$ and a $s\bar{s}$ component and are mixed with the mixing angle φ . Figure 2 shows the $SU(3)_F$ squared matrix elements for meson decays into two pseudoscalar mesons as a function of the scalar mixing angle.

$$\begin{pmatrix} f^H \\ f^L \end{pmatrix} = \begin{pmatrix} \cos \varphi^s & -\sin \varphi^s \\ \sin \varphi^s & \cos \varphi^s \end{pmatrix} \begin{pmatrix} |n\bar{n}\rangle \\ |s\bar{s}\rangle \end{pmatrix} \quad (6)$$

3.5 Supernumerary

The three scalar isoscalar mesons $f_0(1370)$, $f_0(1500)$ and $f_0(1710)$ played an important role in the glueball discussion. Amsler and Close [36,37] suggested to interpret these three states as the result of mixing of the two expected isoscalar states with the scalar glueball.

$$\begin{pmatrix} f_0(1370) \\ f_0(1500) \\ f_0(1710) \end{pmatrix} = \begin{pmatrix} x_{11} & x_{12} & x_{13} \\ x_{21} & x_{22} & x_{23} \\ x_{31} & x_{32} & x_{33} \end{pmatrix} \begin{pmatrix} |n\bar{n}\rangle \\ |s\bar{s}\rangle \\ |gg\rangle \end{pmatrix} \quad (7)$$

These papers led to a large number of follow-up papers, references can be found in Ref. [35]. In all these papers, these three mesons contain the full glueball, $\sum_j x_{ij}^2 = 1$ is imposed. Note that the squared mass difference between $f_0(1370)$ and $f_0(1710)$ is slightly above 1 GeV^2 , the $f_0(1710)$ could also be a radial excitation (and is interpreted as radial excitation below).

3.6 Conclusions

Identifying a glueball is a difficult task. The main argument in favor of a glueball interpretation is an anomalously large production rate in J/ψ decays. It turns out that scalar mesons are organized like pseudoscalar mesons, into mainly singlet and mainly octet mesons. A large production rate of a mainly-octet scalar isoscalar meson in radiative J/ψ decays directly points to a significant glueball content in its wave function. A second argument relies on meson decays into pseudoscalar mesons. In presence of

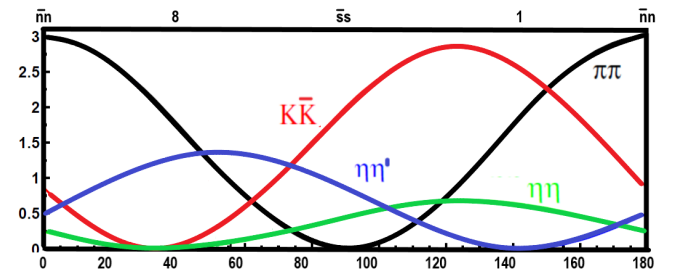


Fig. 2. Decay probabilities of mesons for decays into two pseudoscalar mesons as a function of the scalar mixing angle [35].

a glueball, a pair of mesons assigned to the same multiplet should have a decay pattern that is incompatible with a $q\bar{q}$ interpretation for any mixing angle. Supernumery is a weak argument. It requires a full understanding of the regular excitation spectrum. Further studies are required to learn if central production is gluon-rich. The large production rates of $f_0(1500)$, $f_0(1710)$ and $f_0(2100)$ in $\bar{p}p$ annihilation at collision energies above 3 GeV encourages glueball searches at the FAIR facility with the PANDA detector.

4 Evidence for glueballs from coupled-channel analysis

We have performed a coupled-channel partial wave analysis of radiative J/ψ decays into $\pi^0\pi^0$, $K_s^0 K_s^0$, $\eta\eta$, and $\omega\phi$, constrained by the CERN-Munich data on πN scattering, data from the GAMS collaboration at CERN, data from BNL on $\pi\pi \rightarrow K_s^0 K_s^0$, and 15 Dalitz plots on $\bar{p}p$ annihilation at rest from LEAR. Data on K_{e4} decays constrain the low-energy region. Fitting details and references to the data can be found in Ref. [38].¹ Figure 3 shows the data on radiative J/ψ decays into $\pi^0\pi^0$, $K_s^0 K_s^0$ and the fit. Ten scalar isoscalar resonances were included in the fit. Oller [40] has shown that $f_0(500)$ is singlet-like, the $f_0(980)$ octet-like (see also [41]). The $f_0(1500)$ is seen in Figure 3 as a dip. This pattern was reproduced in Ref. [38] assuming that $f_0(1370)$ is a singlet state and $f_0(1500)$ an octet state. Hence we assumed that the ten mesons can be divided into two series of states, mainly-singlet states with lower masses and mainly-octet states with higher masses.

In a (M^2, n) plot, the masses of singlet and octet states follow two linear trajectories (see Fig. 4). Remarkably, the slope (1.1 GeV^{-2}) is close to the slope of standard Regge trajectories. The separation between the two trajectories is given by the mass square difference between η' and η -meson as suggested by instanton-induced interactions [44]. The figure includes a meson reported by the BESIII collaboration studying $J/\psi \rightarrow \gamma\eta'\eta'$ [45]. As $\eta'\eta'$ resonance, $f_0(2480)$ is very likely a SU(3) singlet state. Indeed, its mass is compatible with the “mainly-singlet” trajectory. The figure gives the pole positions of the eleven resonances as small inserts.

¹ The BESIII data were fitted by Rodas *et al.* [39] with four scalar and three tensor resonances only. I have several objections against the fit. i) It uses an amplitude in which the J/ψ converts into three gluons which hadronize. A final-state meson radiates off the photon. Since the photon is not an isospin eigenstate, this amplitude can produce isovector mesons. This process is highly suppressed and experimentally absent. ii) the $f_0(1370) - f_0(1500)$ interference region is not well described, neither in the mass distribution nor in the $S - D$ phase difference. iii) The fit is neither constrained by the $\pi\pi$ S -wave from the CERN-Munich data nor by the data on K_{e4} decays. A fit with the seven resonances used in Ref. [39] without an isospin breaking amplitude leads to a $\pi\pi$ S -wave that is extremely incompatible with the known $\pi\pi$ S -wave (A.V. Sarantsev, private communication, October 2021.)

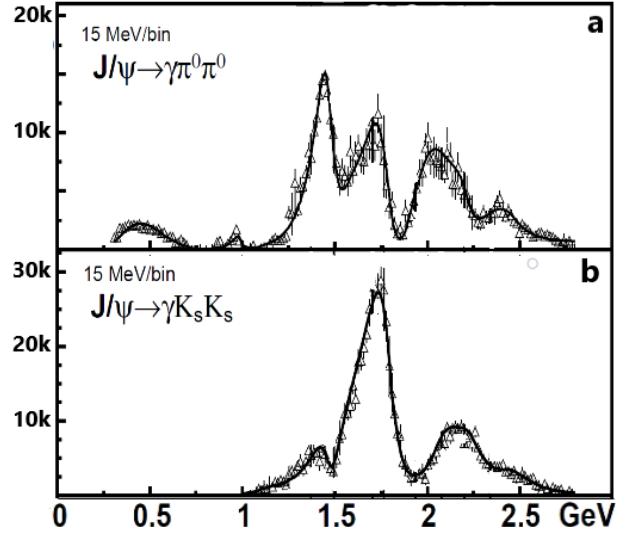


Fig. 3. The squared S -wave transition amplitudes for $J/\psi \rightarrow \pi^0\pi^0$ (a) and $J/\psi \rightarrow K_s^0 K_s^0$ (b). The data points are from an energy-independent partial-wave analysis [42,43], the curve represents our fit [38].

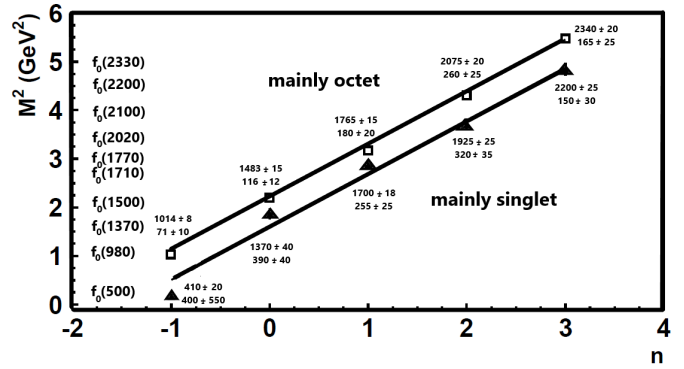


Fig. 4. M^2, n trajectories for mainly-singlet and mainly-octet scalar isoscalar resonances. The red dot at high masses represents a scalar state from $J/\psi \rightarrow \gamma\eta'\eta'$ [45]. Adapted from Ref. [38].

The total yields of scalar mesons in radiative J/ψ decays - including decay modes not reported by the BESIII collaboration - was determined from the coupled-channel analysis [38] that included also other data. The yield of mainly-octet and mainly-singlet mesons as a function of their mass is shown in Fig. 5. Mainly-octet mesons should not be produced (or at most weakly) in radiative J/ψ decays. However, they are produced abundantly, in a limited mass range centered at about 1865 MeV. Mainly-singlet mesons are produced over the full mass range but show a peak structure at the same mass. This enhancement must be due to the scalar glueball mixing into the wave functions of scalar mainly-octet and mainly-singlet mesons. A Breit-Wigner fit to these distributions gives mass and width

$$M_G = (1865 \pm 25^{+10}_{-30}) \text{ MeV} \quad \Gamma_G = (370 \pm 50^{+30}_{-20}) \text{ MeV}, \quad (8)$$

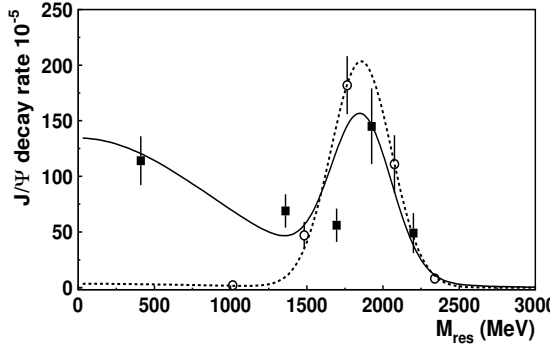


Fig. 5. Yield of scalar isoscalar mesons in radiative J/ψ decays into mainly-octet (open circles) and mainly-singlet mesons (full squares) as a function of their mass [38].

and the (observed) yield is determined to

$$Y_{J/\psi \rightarrow \gamma G} = (5.8 \pm 1.0) 10^{-3}. \quad (9)$$

5 Meson-glueball mixing

Earlier attempts to identify the glueball have in common that the full glueball is distributed among the three states $f_0(1370)$, $f_0(1500)$ and $f_0(1710)$. Inspecting Fig. 3, this seems not to be obvious: Above 1 GeV, four peaks with three valleys are seen, and there is no reason why one particular region should be more gluish than the other ones. The yield of scalar mesons sees the glueball contribution distributed over several resonances.

We did not impose that the full glueball should be seen in these three states nor that we must see the full glueball at all. We fitted the decay modes of pairs of scalar mesons, one mainly-singlet one mainly-octet, and allowed for a glueball component [35].

$$\begin{aligned} f_0^{\text{H}}(xxx) &= (n\bar{n} \cos \varphi_n^s - s\bar{s} \sin \varphi_n^s) \cos \phi_{\text{nH}}^G + G \sin \phi_{\text{nH}}^G \\ f_0^{\text{L}}(xxx) &= (n\bar{n} \sin \varphi_n^s + s\bar{s} \cos \varphi_n^s) \cos \phi_{\text{nL}}^G + G \sin \phi_{\text{nL}}^G \end{aligned} \quad (10)$$

φ_n^s is the scalar mixing angle, ϕ_{nH}^G and ϕ_{nL}^G are the meson-glueball mixing angles of the high-mass state H and of the low-mass state L in the nth nonet. The fractional glueball content of a meson is given by $\sin^2 \phi_{\text{nH}}^G$ or $\sin^2 \phi_{\text{nL}}^G$.

With this mixing scheme and the SU(3) coupling constant (see Fig. 2), we have fitted the meson decay modes and have thus determined the glueball content of the eight high-mass scalar mesons. Figure 6 shows the glueball fraction in the scalar mesons.

The glueball fractions derived from the decay analysis of pairs of scalar mesons add up to a sum that is compatible with 1. The distribution of the glueball fraction in Fig. 6 is identical to the distribution of yields in Fig. 5. This is a remarkable confirmation that the scalar glueball of lowest mass has been identified and has mass and width as given in Eqn. (8) and a yield as given in Eqn. (9).

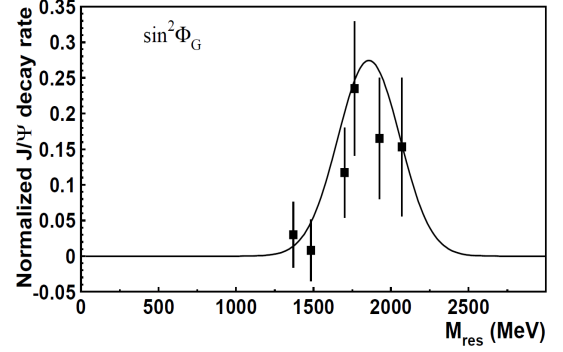


Fig. 6. The glueball content of scalar mesons. Black squares: $\sin^2 \varphi_n^s$, solid curve: Breit-Wigner resonance with area 1 [35].

6 Comparison with LHCb data

Most striking is the mountain landscape above 1500 MeV in the data on radiative J/ψ decays. In these decays a $c\bar{c}$ pair converts into gluons which hadronize (see Fig. 7, left). The huge peak in the $K\bar{K}$ mass spectrum at 1750 MeV and the smaller one at 2100 MeV decay are produced with two gluons in the initial state. This is to be contrasted with data on B_s^0 and \bar{B}_s^0 decays into $J/\psi + \pi^+\pi^-$ [46] and $K\bar{K}$ [47]. In this reaction, a primary $s\bar{s}$ pair – recoiling against the J/ψ – converts into the final state mesons (see Fig. 7, right). We have included the spherical harmonic moments in the coupled channel analysis that describes the radiative J/ψ decays [48]. High-mass scalar mesons are only weakly produced in B_s^0 decays with $s\bar{s}$ in the initial state. The strong peak in the $K\bar{K}$ invariant mass at 1750 MeV in Fig. 3 is nearly absent in $B_s^0 \rightarrow J/\psi K\bar{K}$!

Figure 8 shows the ratio of the decay frequencies of $J/\psi \rightarrow \gamma f_0$ and $B_s^0 \rightarrow J/\psi f_0$ with f_0 decaying into $\pi\pi$ or $K\bar{K}$. The $f_0(980)$ is likely a mainly-octet state, little produced in radiative J/ψ decays but strongly with $s\bar{s}$ in the initial state. On the contrary, $f_0(1770)$ is seen as strong peak in radiative J/ψ but very weakly only in B_s^0 decays. The uncertainties are large, but the ratio of the decay frequencies is fully compatible with the shape of the glueball derived above.

This is highly remarkable: the two gluons in the initial state must be responsible for the production of resonances that decay strongly into $K\bar{K}$ but are nearly absent when $s\bar{s}$ pairs are in the initial state. Also, there is a rich structure in the $\pi\pi$ mass spectrum produced in radiative J/ψ decays but little activity only when the initial state is an $s\bar{s}$ pair: The rich structure stems from gluon-gluon dynamics. Similar conclusions can be drawn [41] from a compari-

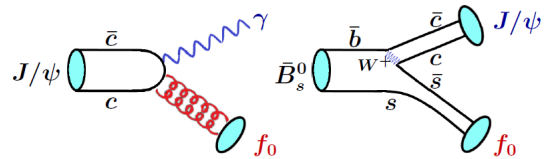


Fig. 7. In radiative J/ψ decays two gluons, in $\bar{B}_s^0 \rightarrow J/\psi + s\bar{s}$, a $s\bar{s}$ pair may convert into a scalar meson.

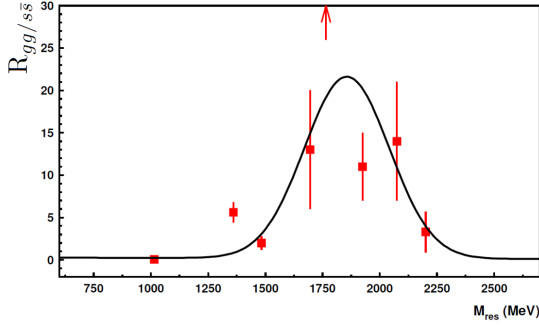


Fig. 8. The ratio $R_{gg/s\bar{s}}$ of the frequencies for $J/\psi \rightarrow \gamma f_0$ and $B_s^0 \rightarrow J/\psi f_0$ with f_0 decaying into $\pi\pi$ or $K\bar{K}$.

son of the invariant mass distributions from radiative J/ψ decays with the pion and kaon form factors [49]. Their square is proportional to the cross sections. The $f_0(980)$ resonance dominates both formfactors but is nearly absent in radiative J/ψ decays: The $f_0(980)$ has large $n\bar{n}$ and $s\bar{s}$ components mixed to a dominant SU(3) octet component. The large intensity above 1500 MeV in radiative J/ψ decays is absent when not two gluons but an $s\bar{s}$ pair is in the initial state: the mountainous structure in radiative J/ψ decays is produced by gluons and not by $q\bar{q}$ pairs: The structure is due to the scalar glueball.

7 A trace of the tensor glueball

The tensor glueball is predicted with an even higher yield [33]:

$$\Gamma_{J/\psi \rightarrow \gamma/G_{2++}}/\Gamma_{\text{tot}} = (11 \pm 2)10^{-3}. \quad (11)$$

The yield of $f_2(1270)$ in radiative J/ψ decays is $(1.64 \pm 0.12)10^{-3}$, about six times weaker than the predicted rate for the tensor glueball! Bose symmetry implies that the $\pi^0\pi^0$ or $K_s K_s$ pairs are limited to even angular momenta, practically, only S and D -waves contribute. The scalar intensity originates from the electric dipole transition $E0$. Three electromagnetic amplitudes $E1$, $M2$, and $E3$ excite tensor mesons. Figure 9 shows these three amplitudes and the relative phases.

Two fits were performed [50]. One fit describes the mass distribution only. Apart from the well known $f_2(1270)$ and $f_2'(1525)$ the fit needs one high-mass resonance with

$$M = (2210 \pm 60) \text{ MeV}; \quad \Gamma = (360 \pm 120) \text{ MeV}, \quad (12)$$

where the error includes systematic studies with or without additional low-yield resonances. The enhancement was called $X_2(2210)$. In this fit, the phases are not well described. Figure 9 shows a fit in which the 2200 MeV region is described by three tensor resonances with masses and widths of about $(M, \Gamma) = (2010, 200)$, $(2300, 150)$, and $(2340, 320)$ MeV. These resonances had been observed by Etkin *et al.* [12] in the reaction $\pi^- p \rightarrow \phi \phi n$. The unusual production characteristics were interpreted in Ref. [12] as evidence that *these states are produced by 1 – 3 glueballs*.

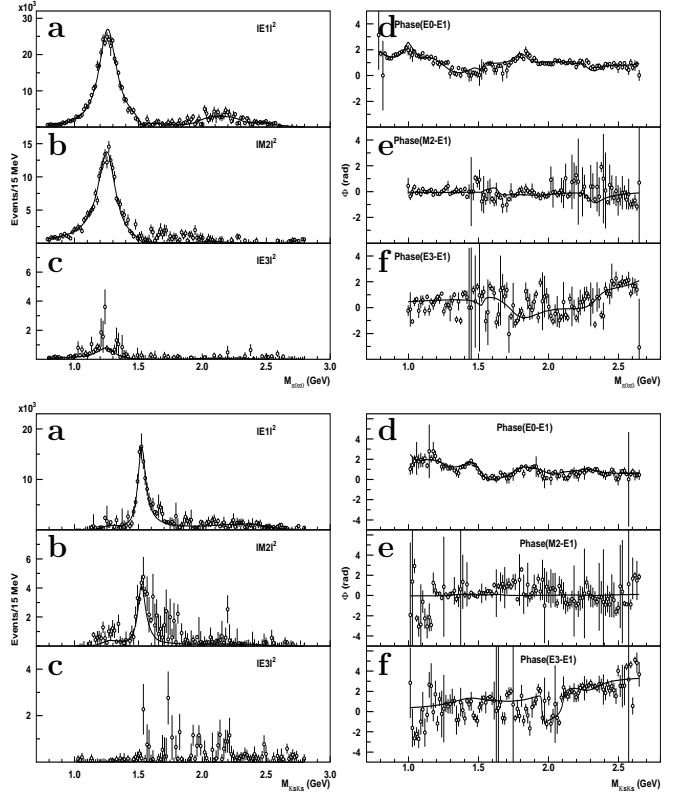


Fig. 9. D -wave intensities and phases for radiative J/ψ decays into $\pi^0\pi^0$ (top subfigures) and $K_s K_s$ (bottom subfigures) from Ref. [42, 43]. The subfigures show the $E1$ (a), $M2$ (b) and $E3$ (c) squared amplitudes and the phase differences between the $E0$ and $E1$ (d) amplitudes, the $M2$ and $E1$ (e) amplitudes, and the $E3$ and $E1$ (f) amplitudes as functions of the meson-meson invariant mass. The phase of the $E0$ amplitude is set to zero. The curve represents our best fit.

The total observed yield of $X_2(2210)$ in $\pi\pi$ and $K\bar{K}$ is $(0.35 \pm 0.15)10^{-3}$, far below the expected glueball yield. We assume the glueball is – like the scalar glueball – distributed over several tensor mesons. Adding up all contributions from tensor states above 1900 MeV seen in radiative J/ψ decays, one obtains

$$\sum_{M=1.9 \text{ GeV}}^{M=2.5 \text{ GeV}} Y_{J/\psi \rightarrow \gamma f_2} = (3.1 \pm 0.6)10^{-3}, \quad (13)$$

which is a large yield even though still below the predicted yield.

8 How to find the pseudoscalar glueball

The BESIII collaboration has studied the reaction $J/\psi \rightarrow \pi^+\pi^-\eta'$ [51]. The left panel of Fig. 10 shows the $\pi^+\pi^-\eta'$ invariant mass distributions with a series of peaks. Assuming that these are all pseudoscalar mesons, two trajectories can be drawn (right panel of Fig. 10). The figure suggests

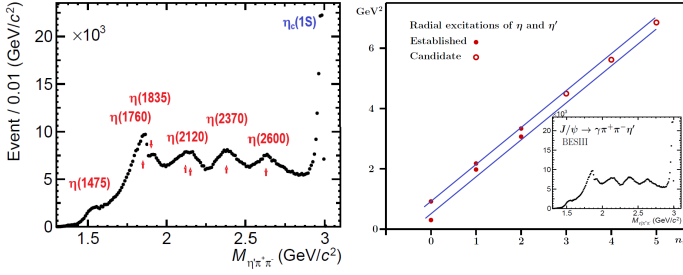


Fig. 10. Left: The $\pi^+\pi^-\eta'$ mass distribution from radiative J/ψ decays [51]. The quantum numbers are not known. Right: M^2 versus n trajectories.

that the higher-mass structures could house two mesons, possibly singlet and octet states in $SU(3)$. If this is true, a cut in the $\pi^+\pi^-$ invariant mass at about 1480 MeV would partly separate the two isobars, $X(2600) \rightarrow f_0(1370)\eta'$ and $X(2600) \rightarrow f_0(1500)\eta'$. We may expect a slight mass shift in the two $\pi^+\pi^-\eta'$ invariant mass distributions. The two mesons $f_0(1370)$ and η' are both mainly singlet. The $f_0(1370)\eta'$ isobar as singlet meson in the $X(2600)$ complex should be slightly higher in mass than the $f_0(1500)\eta'$ mainly octet meson.

The total yields of the high-mass structures – including unseen decay modes – are not known. Nevertheless, their appearance above a comparatively low background is surprising. Personally, I suppose that the pseudoscalar glueball is rather wide, and that the structures are seen so clearly because of a small glueball content. More studies of these data and of different channels are required to substantiate this conjecture.

9 Outlook

The data of the BESIII collaboration presented above are based on $1.3 \cdot 10^9$ events taken at the J/ψ . Presently available are 10^{10} events. Based on this large statistics, rare radiative decays like $J/\psi \rightarrow \gamma\eta\eta'$ [52, 53] and $J/\psi \rightarrow \gamma\eta'\eta'$ [45] have been analysed. Data on the different charge mode of $J/\psi \rightarrow \gamma 4\pi$ would be extremely important. In an ideal world, these data would be publicly available after publication and would be included in different coupled-channel partial-wave analyses.

Radiative decays of $\psi(2S)$ and of $\Upsilon(1S)$ open a wider range in invariant mass. The authors of Ref. [54] used the data of the CLEO collaboration on radiative $\psi(2S)$ decays into $\pi^+\pi^-$ and K^+K^- . The data are shown in Fig. 11. The data are fit with known resonances, no partial-wave analysis was performed. The BaBar collaboration studied radiative $\Upsilon(1S)$ decays into $\pi^+\pi^-$ and K^+K^- [55]. The results are shown in Fig. 12. In all four distributions, there is not a single prominent peak in the S -wave contribution which would stick out as glueball candidate. The S -waves rather resembles the distributions observed in radiative J/ψ : three major enhancement in the 1500, 1750 and 2200 MeV region separated by dips. (With the

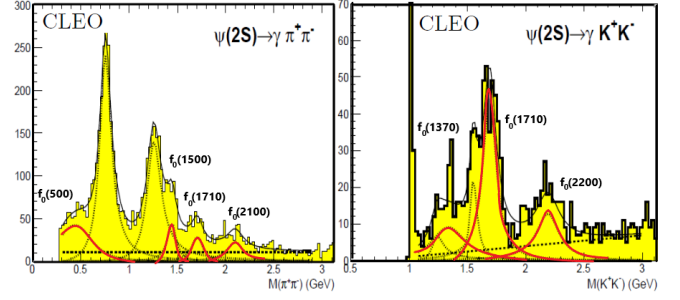


Fig. 11. $\pi^+\pi^-$ (left) and K^+K^- (right) invariant mass distributions from radiative decays of $\psi(2S)$. The red curves represent the S -wave contributions. Adapted from [54].

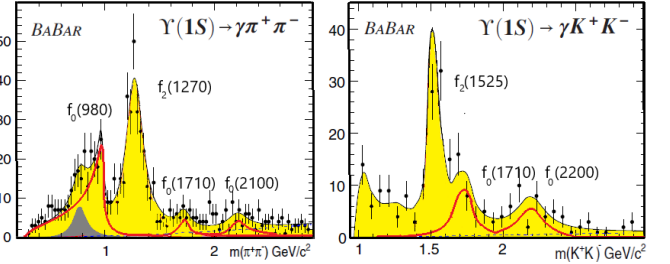


Fig. 12. $\pi^+\pi^-$ (left) and K^+K^- (right) invariant mass distributions from radiative decays of $\Upsilon(1S)$. The $\Upsilon(1S)$ is observed in $\Upsilon(2S)/\Upsilon(3S) \rightarrow \pi^+\pi^-\Upsilon(1S)$. The red curves represent the S -wave contributions, the grey area the $\rho(770)$ contribution. Adapted from [55].

larger statistics in J/ψ decays, a fourth enhancement is seen at about 2350 MeV.) In Fig. 11, a peak is found at 1447 MeV and assigned to $f_0(1500)$. At 1500 MeV, there is the dip. The wrong mass is due to the neglect of interference: The phase between $f_0(1500)$ and the “background” (due to the wider $f_0(1370)$) is 180° [38]. This phase difference and the significant $f_0(1500) \rightarrow \eta\eta'$ branching ratio identify $f_0(1500)$ as mainly $SU(3)_F$ octet state. The different masses for the high-mass state in the $\pi^+\pi^-$ and K^+K^- invariant mass distributions point again to the neglect of interference between the prominent octet states and the singlet “background”. Inspecting Figs. 11 and 12 shows: there is no striking isolated peak which could be interpreted as “the glueball”. The glueball content must be distributed over a large number of states.

In $\psi(2S)$ radiative decays, the $f_0(1710) \rightarrow K\bar{K}$ is observed with a branching fraction of $(6.7 \pm 0.9) \cdot 10^{-5}$, in $\Upsilon(1S)$ radiative decays, the $f_0(1710) \rightarrow K^+K^-$ is seen with a branching ratio of $(2.02 \pm 0.51 \pm 0.35) \cdot 10^{-5}$. The comparison with the yield observed in Ref. [38] allows us to calculate the branching ratio expected for $\psi(2S)$ and $\Upsilon(1S)$ decays when the full scalar glueball is covered, i.e. for $\Upsilon(1S) \rightarrow \gamma G_0(1865)$. The values are given in Table 2.

Clearly, a significant increase in statistics is required when these reactions should make an independent impact. The advantage of $\psi(2S)$ and $\Upsilon(1S)$ radiative decays is of course that phase space limitations play no role any more. This is particularly important for the search for the tensor

Table 2. Radiative yields expected for $\psi(2S)$ and $\Upsilon(1S)$ radiative decays into the scalar glueball.

	“Exp.”	Theory	Ref.
$\psi(2S) \rightarrow \gamma G_0(1865)$	$\sim 5 \cdot 10^{-4}$	$(5.9^{+3.4}_{-1.4}) \cdot 10^{-4}$	[56]
$\Upsilon(1S) \rightarrow \gamma G_0(1865)$	$\sim 3 \cdot 10^{-4}$	$(1.3^{+0.7}_{-0.3}) \cdot 10^{-4}$	[56]
		$(1 - 2) \cdot 10^{-3}$	[57]

and pseudoscalar glueball. The scalar glueball seems to be confirmed: there is not much intensity above 2500 MeV.

At the end I would like to give an answer to the question posed in the title: yes, I am convinced, the scalar glueball is identified, and the tensor glueball seems to have left first traces in the data.

References

1. C. A. Heusch, “Gluonium: An Unfulfilled promise of QCD?,” in *Workshop on QCD: 20 Years Later*, pp. 555–574, 11 1992.
2. H. Fritzsch and M. Gell-Mann, “Current algebra: Quarks and what else?,” *eConf*, vol. C720906V2, pp. 135–165, 1972.
3. H. Fritzsch, M. Gell-Mann, and H. Leutwyler, “Advantages of the Color Octet Gluon Picture,” *Phys. Lett. B*, vol. 47, pp. 365–368, 1973.
4. J. E. Augustin *et al.*, “Discovery of a Narrow Resonance in e^+e^- Annihilation,” *Phys. Rev. Lett.*, vol. 33, pp. 1406–1408, 1974.
5. D. L. Scharre *et al.*, “Observation of the Radiative Transition $\psi \rightarrow \gamma E(1420)$,” *Phys. Lett. B*, vol. 97, pp. 329–332, 1980.
6. C. Edwards *et al.*, “Observation of a Pseudoscalar State at 1440-MeV in J/ψ Radiative Decays,” *Phys. Rev. Lett.*, vol. 49, p. 259, 1982. [Erratum: *Phys.Rev.Lett.* 50, 219 (1983)].
7. R. L. Jaffe and K. Johnson, “Unconventional States of Confined Quarks and Gluons,” *Phys. Lett. B*, vol. 60, pp. 201–204, 1976.
8. C. Edwards *et al.*, “Observation of an $\eta\eta$ Resonance in J/ψ Radiative Decays,” *Phys. Rev. Lett.*, vol. 48, p. 458, 1982.
9. W. Dunwoodie, “ J/ψ radiative decay to two pseudoscalar mesons from MARK III,” *AIP Conf. Proc.*, vol. 432, no. 1, pp. 753–757, 1998.
10. F. G. Binon *et al.*, “ $G(1590)$: A Scalar Meson Decaying Into Two η Mesons,” *Nuovo Cim. A*, vol. 78, p. 313, 1983.
11. A. Etkin *et al.*, “The Reaction $\pi^- p \rightarrow \phi\phi n$ and Evidence for Glueballs,” *Phys. Rev. Lett.*, vol. 49, p. 1620, 1982.
12. A. Etkin *et al.*, “Increased Statistics and Observation of the $g(T)$, g'_T , and g''_T 2^{++} Resonances in the Glueball Enhanced Channel $\pi^- p \rightarrow \phi\phi n$,” *Phys. Lett. B*, vol. 201, pp. 568–572, 1988.
13. E. Klempt *Phys. Lett. B*, vol. 308, pp. 179–185, 1993.
14. E. Klempt, C. Batty, and J.-M. Richard, “The Antinucleon-nucleon interaction at low energy : Annihilation dynamics,” *Phys. Rept.*, vol. 413, pp. 197–317, 2005.
15. K. Johnson, “The M.I.T. Bag Model,” *Acta Phys. Polon. B*, vol. 6, p. 865, 1975.
16. D. Robson, “A Basic Guide for the Glueball Spotter,” *Nucl. Phys. B*, vol. 130, pp. 328–348, 1977.
17. Y. Chen *et al.*, “Glueball spectrum and matrix elements on anisotropic lattices,” *Phys. Rev. D*, vol. 73, p. 014516, 2006.
18. A. Athenodorou and M. Teper, “The glueball spectrum of $SU(3)$ gauge theory in 3 + 1 dimensions,” *JHEP*, vol. 11, p. 172, 2020.
19. E. Gregory, A. Irving, B. Lucini, C. McNeile, A. Rago, C. Richards, and E. Rinaldi, “Towards the glueball spectrum from unquenched lattice QCD,” *JHEP*, vol. 10, p. 170, 2012.
20. A. P. Szczepaniak and E. S. Swanson, “The Low lying glueball spectrum,” *Phys. Lett. B*, vol. 577, pp. 61–66, 2003.
21. H.-X. Chen, W. Chen, and S.-L. Zhu, “Two- and three-gluon glueballs of $C = +$,” *Phys. Rev. D*, vol. 104, no. 9, p. 094050, 2021.
22. M. Q. Huber, C. S. Fischer, and H. Sanchis-Alepuz, “Higher spin glueballs from functional methods,” *Eur. Phys. J. C*, vol. 81, no. 12, p. 1083, 2021. [Erratum: *Eur.Phys.J.C* 82, 38 (2022)].
23. M. Q. Huber, C. S. Fischer, and H. Sanchis-Alepuz, “Spectrum of scalar and pseudoscalar glueballs from functional methods,” *Eur. Phys. J. C*, vol. 80, no. 11, p. 1077, 2020.
24. M. Rinaldi and V. Vento, “Meson and glueball spectroscopy within the graviton soft wall model,” *Phys. Rev. D*, vol. 104, no. 3, p. 034016, 2021.
25. H. J. Rothe, vol. 82 (2012). World Scientific Publishing Company, 2012.
26. C. J. Morningstar and M. J. Peardon, “The Glueball spectrum from an anisotropic lattice study,” *Phys. Rev. D*, vol. 60, p. 034509, 1999.
27. J. Ruiz de Elvira, J. R. Pelaez, M. R. Pennington, and D. J. Wilson, “Chiral Perturbation Theory, the $1/N_c$ expansion and Regge behaviour determine the structure of the lightest scalar meson,” *Phys. Rev. D*, vol. 84, p. 096006, 2011.
28. S. Narison, “Masses, decays and mixings of gluonia in QCD,” *Nucl. Phys. B*, vol. 509, pp. 312–356, 1998.
29. J. Sexton, A. Vaccarino, and D. Weingarten, “Coupling constants for scalar glueball decay,” *Nucl. Phys. B Proc. Suppl.*, vol. 47, pp. 128–135, 1996.
30. M. Iwasaki, S.-I. Nawa, T. Sanada, and F. Takagi, “A Flux tube model for glueballs,” *Phys. Rev. D*, vol. 68, p. 074007, 2003.
31. P. Bicudo, S. R. Cotanch, F. J. Llanes-Estrada, and D. G. Robertson, “The BES $f_0(1810)$: A New Glueball Candidate,” *Eur. Phys. J. C*, vol. 52, pp. 363–374, 2007.
32. L.-C. Gui, Y. Chen, G. Li, C. Liu, Y.-B. Liu, J.-P. Ma, Y.-B. Yang, and J.-B. Zhang, “Scalar Glueball in Radiative J/ψ Decay on the Lattice,” *Phys. Rev. Lett.*, vol. 110, no. 2, p. 021601, 2013.
33. Y. Chen, L.-C. Gui, G. Li, C. Liu, Y.-B. Liu, J.-P. Ma, Y.-B. Yang, and J.-B. Zhang, “Glueballs in charmonia radiative decays,” *PoS*, vol. LATTICE2013, p. 435, 2014.
34. L.-C. Gui, J.-M. Dong, Y. Chen, and Y.-B. Yang, “Study of the pseudoscalar glueball in J/ψ radiative decays,” *Phys. Rev. D*, vol. 100, no. 5, p. 054511, 2019.
35. E. Klempt and A. V. Sarantsev, “Singlet-octet-glueball mixing of scalar mesons,” *Phys. Lett. B*, vol. 826, p. 136906, 2022.
36. C. Amsler and F. E. Close, “Evidence for a scalar glueball,” *Phys. Lett. B*, vol. 353, pp. 385–390, 1995.
37. C. Amsler and F. E. Close, “Is $f_0(1500)$ a scalar glueball?,” *Phys. Rev. D*, vol. 53, pp. 295–311, 1996.

38. A. V. Sarantsev, I. Denisenko, U. Thoma, and E. Klempt, “Scalar isoscalar mesons and the scalar glueball from radiative J/ψ decays,” *Phys. Lett. B*, vol. 816, p. 136227, 2021.
39. A. Rodas, A. Pilloni, M. Albaladejo, C. Fernandez-Ramirez, V. Mathieu, and A. P. Szczepaniak, “Scalar and tensor resonances in J/ψ radiative decays,” *Eur. Phys. J. C*, vol. 82, no. 1, p. 80, 2022.
40. J. A. Oller, “The Mixing angle of the lightest scalar nonet,” *Nucl. Phys. A*, vol. 727, pp. 353–369, 2003.
41. E. Klempt, “Scalar mesons and the fragmented glueball,” *Phys. Lett. B*, vol. 820, p. 136512, 2021.
42. M. Ablikim *et al.*, “Amplitude analysis of the $\pi^0\pi^0$ system produced in radiative J/ψ decays,” *Phys. Rev. D*, vol. 92, no. 5, p. 052003, 2015. [Erratum: *Phys. Rev. D* 93, 039906 (2016)].
43. M. Ablikim *et al.*, “Amplitude analysis of the $K_S K_S$ system produced in radiative J/ψ decays,” *Phys. Rev. D*, vol. 98, no. 7, p. 072003, 2018.
44. E. Klempt, B. C. Metsch, C. R. Munz, and H. R. Petry, “Scalar mesons in a relativistic quark model with instanton induced forces,” *Phys. Lett. B*, vol. 361, pp. 160–166, 1995.
45. M. Ablikim *et al.*, “Partial wave analysis of $J/\psi \rightarrow \gamma\eta'\eta'$,” 2022.
46. R. Aaij *et al.*, “Measurement of resonant and CP components in $\bar{B}_s^0 \rightarrow J/\psi\pi^+\pi^-$ decays,” *Phys. Rev. D*, vol. 89, no. 9, p. 092006, 2014.
47. R. Aaij *et al.*, “Resonances and CP violation in B_s^0 and $\bar{B}_s^0 \rightarrow J/\psi K^+ K^-$ decays in the mass region above the $\phi(1020)$,” *JHEP*, vol. 08, p. 037, 2017.
48. A. V. Sarantsev and E. Klempt, “Scalar and tensor mesons in $d\bar{d}$, $s\bar{s}$ and $gg \rightarrow f_0, f_2$,” 11, 2022.
49. S. Ropertz, C. Hanhart, and B. Kubis, “A new parametrization for the scalar pion form factors,” *Eur. Phys. J. C*, vol. 78, no. 12, p. 1000, 2018.
50. E. Klempt, K. V. Nikonov, A. V. Sarantsev, and I. Denisenko, “Search for the tensor glueball,” *Phys. Lett. B*, vol. 830, p. 137171, 2022.
51. M. Ablikim *et al.*, “Observation of a State $X(2600)$ in the $\pi^+\pi^-\eta'$ System in the Process $J/\psi \rightarrow \gamma\pi^+\pi^-\eta'$,” *Phys. Rev. Lett.*, vol. 129, no. 4, p. 042001, 2022.
52. M. Ablikim *et al.*, “Partial wave analysis of $J/\psi \rightarrow \gamma\eta\eta'$,” *Phys. Rev. D*, vol. 106, no. 7, p. 072012, 2022.
53. M. Ablikim *et al.*, “Observation of an isoscalar resonance with exotic $J^{PC} = 1^{-+}$ quantum numbers in $J/\psi \rightarrow \gamma\eta\eta'$,” 2 2022.
54. S. Dobbs, A. Tomaradze, T. Xiao, and K. K. Seth, “Comprehensive Study of the Radiative Decays of J/ψ and $\psi(2S)$ to Pseudoscalar Meson Pairs, and Search for Glueballs,” *Phys. Rev. D*, vol. 91, no. 5, p. 052006, 2015.
55. J. P. Lees *et al.*, “Study of $\Upsilon(1S)$ radiative decays to $\gamma\pi^+\pi^-$ and $\gamma K^+ K^-$,” *Phys. Rev. D*, vol. 97, no. 11, p. 112006, 2018.
56. R. Zhu, “Factorization for radiative heavy quarkonium decays into scalar Glueball,” *JHEP*, vol. 09, p. 166, 2015.
57. X. G. He, H. Y. Jin, and J. P. Ma, “Radiative decay of Υ into a scalar glueball,” *Phys. Rev. D*, vol. 66, p. 074015, 2002.